



Dalton  
Transactions

**Europium Doping of Cadmium Selenide (CdSe) Quantum Dots via Rapid Microwave Synthesis for Optoelectronic Applications**

Journal:	<i>Dalton Transactions</i>
Manuscript ID	DT-ART-08-2021-002920.R2
Article Type:	Paper
Date Submitted by the Author:	29-Nov-2021
Complete List of Authors:	Thomas, Donovan; Norfolk State University Lee, Harold; Sandia National Laboratories, Advanced Materials Laboratory Santiago, Kevin; Norfolk State University Pelzer, Marvin; Norfolk State University Kuti, Ayodeji; Norfolk State University Treadwell, LaRico; Sandia National Laboratories, Nanomaterials and Inorganic chemistry Bahoura, Messaoud; Norfolk State University

SCHOLARONE™  
Manuscripts

# Europium Doping of Cadmium Selenide (CdSe) Quantum Dots via Rapid Microwave Synthesis for Optoelectronic Applications

Donovan Thomas,<sup>1</sup> Harold O. Lee III,<sup>3,b</sup> Kevin C. Santiago,<sup>1,2</sup> Marvin Pelzer,<sup>2</sup> Ayodeji Kuti,<sup>2</sup> and LaRico J. Treadwell<sup>3</sup>, and Messaoud Bahoura,<sup>1,2,a</sup>

<sup>1</sup>Center for Materials Research, Norfolk State University, Norfolk, Virginia 23504, USA

<sup>2</sup>Department of Engineering, Norfolk State University, Norfolk, Virginia 23504, USA

<sup>3</sup>Sandia National Laboratories, Advanced Materials Laboratory, Albuquerque, New Mexico 87106, USA

<sup>a</sup>Correspondence and requests for materials can be addressed to Messaoud Bahoura (email: mbahoura@nsu.edu)

<sup>b</sup>Correspondence and requests for materials can be addressed to Harold Lee (email: holee@sandia.gov)

## ABSTRACT

The tunability of optical properties in inorganic semiconductor quantum dots (QDs) allows them to be exceptional candidates for multiple optical and optoelectronic applications. While QD size dictates these properties, the addition of highly luminescent rare-earth elements also affects absorption and emission properties. In this work, we were able to successfully synthesize europium-doped CdSe QDs using a one-pot microwave synthesis method. Using recipes that we previously developed, we were able to synthesize Eu<sup>3+</sup>:CdSe quantum dots and tune their optical properties by varying microwave irradiation temperatures, hold times, and dopant concentration. UV-Vis spectroscopy and photoluminescence data show that structural incorporation of europium has an effect on the optical properties of CdSe QDs via energy transfer from host to dopant. Eu<sup>3+</sup>:CdSe QDs have diameters ranging from 4.6-10.0 nm and colors ranging from blue-green to dark red. The development of recipes for high throughput rapid microwave synthesis allows for QDs to be synthesized with repeatability, tunability, and scalability.

## 1. INTRODUCTION

In recent years, nanoparticles have gained considerable interest due to their unique properties that differ from their bulk counterparts resulting from their size and composition [1]. These unique properties have led to widespread applications ranging from drug delivery, manufacturing, sunscreens, and anti-fading agents in clothing [2]. A specific subset of nanoparticles called quantum dots (QDs) has seen great interest in optical and optoelectronic applications due to their tailorable absorption and emission properties throughout the visible spectrum via size control. QDs are crystalline nanoparticles in which their radius is smaller than the Bohr radius of the bulk material (typically between 2-20 nm). One of the most well-researched QD systems is cadmium

selenide (CdSe), which has well-known optical properties that are tunable via particle diameter. To further tune their optical properties, CdSe QDs can be doped with metal ions, but these metals need to have specific properties to effectively contribute to the absorption and emission characteristics of the host CdSe QDs [3-7]. Previous literature reports two mechanisms in which doping colloidal QDs with metal ions can occur: structural incorporation or surface attachment [8-10]. The doping mechanism depends on numerous variables such as the chemical properties of the host and dopant material, synthesis conditions, valance state, and ionic radii of the host and dopant [11-15]. Techniques such as UV-visible spectroscopy and photoluminescence can distinguish between the mechanism via the change in their absorption and photoluminescence properties [16-18]. For optical applications, the surface attachment mechanism is not desired because the dopant does not affect the band edge shape or alignment of the host due to ineffective penetration into the QD lattice [19-23]. Structural incorporation on the other hand is desired because the resultant changes to the electronic band structure and band edges cause changes to the optical properties [20-21].

In this work, CdSe QDs were doped with  $\text{Eu}^{3+}$  using the one-pot microwave synthesis method detailed in our previous study [24]. First, the successful fabrication of QDs via rapid microwave synthesis is demonstrated. Next, the ability to tune QD size is demonstrated through systematic studies of microwave synthesis conditions and dopant concentration. Lastly, optical spectroscopy quantified the change in the optical properties of the QDs as a function of size and dopant concentration. Based on the changes in absorption and emission properties it was determined that doping with  $\text{Eu}^{3+}$  leads to structural incorporation into the QDs [9-10]. The development of various recipes and doping concentrations lead to QD emissions ranging from blue-green to deep red. Results show that the one-pot microwave synthesis method leads to QDs of similar quality to those

synthesized via the traditional “hot injection method” but without the inherent health risks and byproducts.

## **2. EXPERIMENTAL METHODS**

### **2.1 Materials**

All materials were used as received from their respective vendors. Oleic acid (tech, 90%), 1-octadecene (technical grade, 90%), selenium powder (-325 mesh, wt. 99.5%), and toluene (ACS, 99.5%) were purchased from Alfa Aesar. Europium (III) acetate hydrate (99.999% trace metal basis), cadmium oxide (CdO) powder (99.5 wt. %), tri-n-octylphosphine (97% TOP), and acetone were purchased from Sigma-Aldrich, Strem Chemicals, and VWR Analytical, respectively.

### **2.2 Precursor Preparation**

The “Eu<sup>3+</sup>:Cd precursor solution” was prepared in an N<sub>2</sub> glovebox by adding 100 mL of 1-octadecene, 6 mL of oleic acid, 130 mg of CdO, and a large stir bar to a 250 mL round bottom flask. The Eu<sup>3+</sup>:Cd precursor solution was taken out of the glovebox and heated to 300 °C under stirring on a hotplate until CdO powder fully dissolved resulting in the precursor solution changing from color brown to clear. The Eu<sup>3+</sup>:Cd precursor solution was allowed to cool to room temperature before proceeding to the next step. Once cooled, Eu<sup>3+</sup>:Cd precursor solution was transferred into the glovebox, and europium (III) acetate hydrate was added. Varying amounts of europium (III) acetate hydrate were added to create 0.025%, 0.05% and 0.1% Eu<sup>3+</sup> doped Cd precursor solutions. Eu<sup>3+</sup>:Cd precursor solution was then removed from the glovebox and heated to no higher than 300 °C under stirring on a hotplate until all europium (III) acetate hydrate powder was dissolved. Note that temperatures higher than 300 °C will cause europium (III) acetate hydrate to decompose into europium oxide, which is not desired. Once dissolved, the Eu<sup>3+</sup>:Cd precursor

solution was allowed to cool to room temperature. The trioctylphosphine selenide (TOP-Se) precursor solution was prepared by adding 300 mg of Se powder, 50 mL of 1-octadecene, 4 mL of TOP, and a large stir bar to a 250 mL round bottom flask and heating to 250 °C under stirring on a hotplate until Se powder fully dissolved. Once dissolved, the TOP-Se precursor solution was allowed to cool to room temperature and then placed inside the glove box.

### 2.3 Synthesis of Quantum Dots

A recipe for one-pot microwave synthesis was adopted and modified from a conventional, “hot-injection” synthesis method that utilizes a three-neck round bottom flask and heating mantle under an inert gas atmosphere. For QD synthesis, the same process discussed in previous studies was used [24]. Power and stirring rotation per minute (RPM) for all samples were kept constant at 300 W and 600 RPM, respectively. The Anton Paar G40 borosilicate glass vial with a maximum reaction volume of 20 mL was used for all samples throughout this study. In the glove box, 10.6 mL of  $\text{Eu}^{3+}$ :Cd precursor solution and 1 mL of TOP-Se precursor solution were added to the reaction vial with a magnetic stir bar. A septum top with a ruby thermometer immersion tube was snapped to the top of the vial to seal the mixture of chemicals inside of the vial. The vial was then taken out of the glove box and added to the Anton Paar Monowave 300 microwave reactor cavity. Time and temperature recipes for specific photoluminescence (PL) wavelengths were then loaded into the Monowave software and the synthesis was carried out with accurate ruby thermometer temperature monitoring. Temperatures and times are shown in Table 1 and are labeled by recipe number.

**Table 1.** Temperature and hold time combinations for microwave recipes.

<b>Recipe</b>	<b>Temperature (°C)</b>	<b>Hold Time (min)</b>
<b>#1</b>	150 °C	3:30
<b>#2</b>	175 °C	1:30
<b>#3</b>	225 °C	0:30
<b>#4</b>	225 °C	5:00
<b>#5</b>	280 °C	4:00

The resulting quantum dot colloidal solutions were transferred into the glove box and divided evenly into centrifuge tubes. Each tube was filled with excess acetone until the tube had a total of 30 mL of solution. Samples were taken out of the glove box and placed into a Beckman Coulter Allegra 25R Centrifuge and centrifuged at 10,000 RPM for 15 minutes. Solutions were vortex mixed with a VWR Analog Vortex Mixer for 10 seconds each. This washing process was repeated until the acetone was as clear as possible. After acetone washing, centrifuge tubes were transferred back into the glove box. Acetone was decanted off and toluene was added to resuspend QDs. The samples were then vortex mixed and centrifuged at 6,000 RPM for 5 minutes. Solvent was decanted off and resuspended in toluene for final storage. The final QD solutions were transferred back into the glove box and stored in amber vials for characterization. Samples are denoted by their synthesis recipe and doping percentage (i.e. #1-0.025%).

#### **2.4 Characterization Techniques.**

UV/Vis spectroscopy was conducted using a Perkin Elmer Lambda 1050 Spectrometer from 400-700 nm using an InGaAs detector at 1 nm increments. Photoluminescence was conducted using a Jobin Yvon Horiba FluoroMax 3 Spectrometer with an excitation wavelength of 400 nm. Photos of CdSe quantum dots were taken under both ambient light and under 365 nm long wavelength UV light.

### 3. RESULTS AND DISCUSSION

#### 3.1. Doping by Percentage

For 0.025%  $\text{Eu}^{3+}$  doped QDs, UV-Vis data in Figure 1a shows red shifting in the absorbance maxima corresponding to a decrease in the optical energy gap attributed to an increase in QD radius [25,26]. QDs synthesized at 150 °C had similar radii as undoped CdSe while increasing reaction temperature led to larger diameters. The greatest increase in QD diameter for 0.025%  $\text{Eu}^{3+}$ :CdSe occurred with recipe #5 with an increase of 3.6 nm which has the highest reaction temperature. QD diameter increases from 6.0 nm to 6.6 nm when the reaction temperature is kept constant while the reaction time is increased as seen in recipes #3 and #4. This suggests that higher temperatures and longer reaction times synergistically cause an increase in nanocrystal growth. Under 365 nm UV light, colors ranging from blue-green to red were produced under the same processing conditions mentioned above, Figure 1c. Figure 1d displays the PL spectra for 0.025%  $\text{Eu}^{3+}$ :CdSe QDs which ranges from 513-634 nm, this is a 25 nm red shift in emission range in comparison to previous studies [24,27]. Using the Brus Approximation equation, the QD diameter were approximated and listed below in Table 2 [28]. As QD diameter increases and shift closer to the Bohr radius of CdSe, they reach weak confinement, which explains the quenching in emission intensity [29,30].

For 0.05%  $\text{Eu}^{3+}$  doped QDs, the UV-Vis data in Figure 1c shows red shifting in the absorbance maxima corresponding to a decrease in the optical energy gap attributed to an increase in QD radius. In comparison to #5-0.025%, #5-0.05% has a greater red shift corresponding to a smaller optical energy gap and subsequently a larger QD diameter. Also, a 34 nm and 12 nm red-shifts were observed for #3-0.05% and 0.025% when compared to literature (undoped), respectively [24]. As seen in Figure 2 under 365 nm UV light, colors ranging from blue-green to

dark red were produced corresponding to PL wavelengths ranging from 521- 647 nm for the same time and temperature combinations discussed throughout this manuscript. The observed redshift ranges from 8 nm to 15 nm versus the PL recipes of the 0.025% doped QDs. These shifts in wavelengths theoretically represent larger quantum dots, shifting closer to the weak confinement region which would account for the visual decrease in brightness and quenching in fluorescence for longer emission wavelength QD's at this doping percentage. For shorter wavelengths (521 nm and 542 nm), QDs remain in the strong confinement regime as indicated by strong PL intensities. Using Brus approximation, calculated diameters for 0.05%  $\text{Eu}^{3+}$ :CdSe QDs increased compared to undoped and 0.025% doping. For smaller QDs, a 4% increase in diameter was calculated whereas for larger QDs a 12 % increase in diameter size when doped with 0.05%  $\text{Eu}^{3+}$ . Table 2 shows the PL wavelength peaks and corresponding calculated diameters for 0.05%  $\text{Eu}^{3+}$ :CdSe QDs.

For 0.1%  $\text{Eu}^{3+}$  doped QDs, UV-VIS data in Figure 1e also shows similar ranges in optical absorption for 0.1%  $\text{Eu}^{3+}$ :CdSe when compared to 0.05% doping, with very small red shifts in absorption maxima. When viewing the QDs under 365 nm UV light, colors ranging from yellow to dark red corresponding to PL wavelengths ranging from 528- 656 nm for the 5 recipes. The observed redshift ranges from 2 nm to 9 nm versus the PL recipes of the 0.05% doped QDs. Note the weak PL intensity at 656 nm is due to large QDs approaching weak confinement. The appearance of PL peaks near 592 nm and 616 nm became more pronounced at this doping level, which is attributed to europium (III) acetate hydrate which is explained later in this manuscript. Calculated radii presented in Table 3 show that #5-0.1% leads to QDs with diameters at the lower limit of the reported CdSe Bohr radius as indicated by their low PL intensity [29-31]. A full head-to-head comparison between doping percentages can be found Tables 2-3.



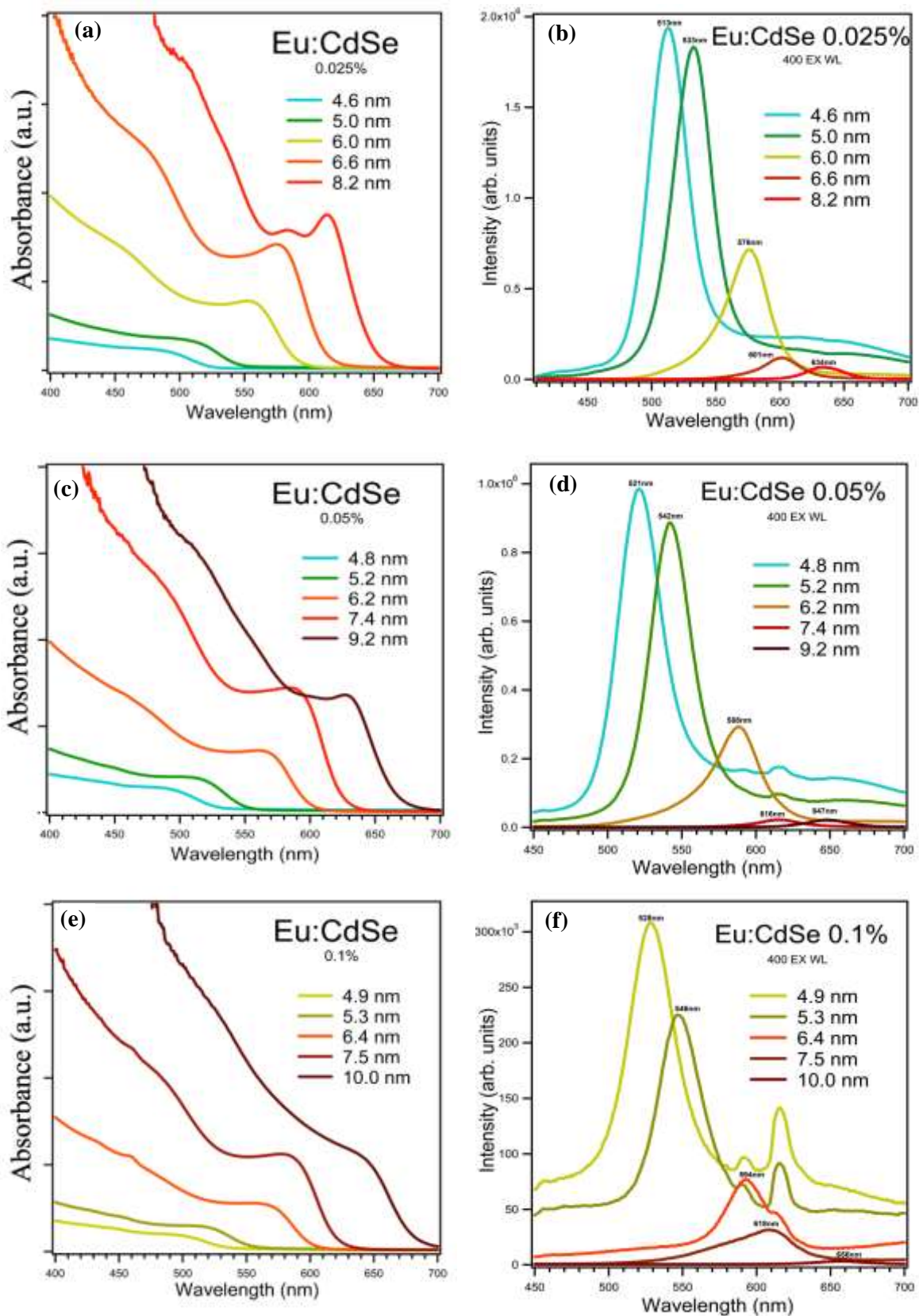


**Figure 1.** (a) UV-Vis spectra and (b) PL spectra of 0.025% doped Eu<sup>3+</sup>:CdSe QDs, (c) UV-Vis spectra and (d) PL spectra of 0.05% doped Eu<sup>3+</sup>:CdSe QDs, and (e) UV-Vis spectra and (f) PL spectra of 0.1% doped Eu<sup>3+</sup>:CdSe QDs.

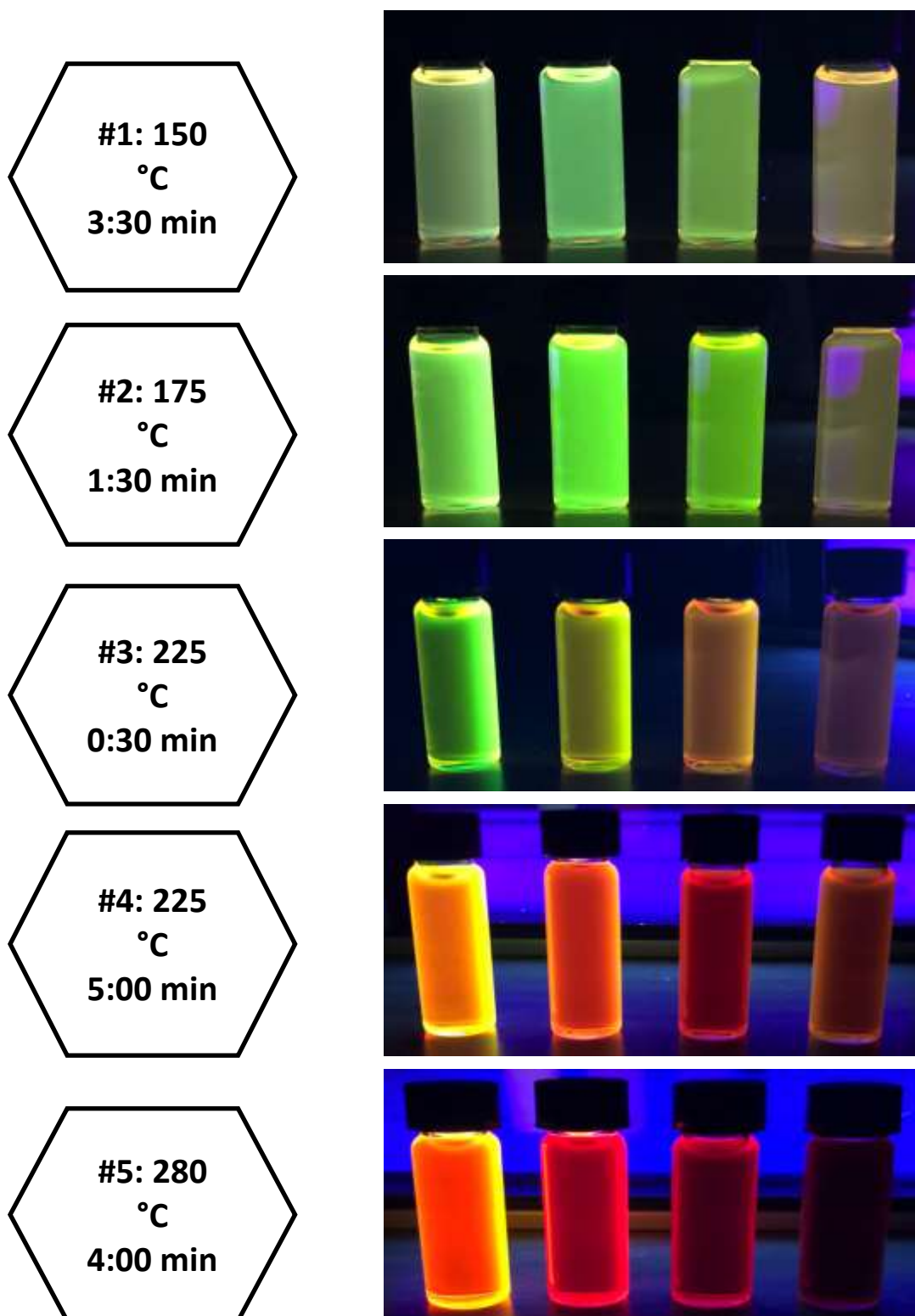


**Figure 2.** CdSe colloidal quantum dots in increasing order of europium doping from undoped, 0.025%, 0.05%, to 0.1% (left to right) under 365 nm UV light. Undoped and 0.025% CdSe displays the brightest fluorescence. These images correspond to Tables 1-2.

**Table 2.** PL wavelength for each time and temperature combination as doping increases for  $\text{Eu}^{3+}:\text{CdSe}$  quantum dots

Recipe #	0%	0.025% $\text{Eu}^{3+}$	0.05% $\text{Eu}^{3+}$	0.1% $\text{Eu}^{3+}$
1	509 nm	513 nm	521 nm	528 nm
2	523 nm	533 nm	542 nm	546 nm
3	554 nm	576 nm	588 nm	594 nm
4	581 nm	601 nm	616 nm	618 nm
5	605 nm	634 nm	647 nm	656 nm

**Table 3.** QD diameter for each time and temperature combination as europium doping increases.

Recipe #	0%	0.025% $\text{Eu}^{3+}$	0.05% $\text{Eu}^{3+}$	0.1% $\text{Eu}^{3+}$
1	4.6 nm	4.6 nm	4.8 nm	4.9 nm
2	4.8 nm	5.0 nm	5.2 nm	5.3 nm
3	5.4 nm	6.0 nm	6.2 nm	6.4 nm
4	6.2 nm	6.6 nm	7.4 nm	7.5 nm
5	6.8 nm	8.2 nm	9.2 nm	10 nm

### 3.2 Doping by Time and Temperature

Figures 3-7 present direct comparisons of QDs by overlaying the various doping percentages for each recipe with UV/Vis spectra on the left and PL spectra on the right. Synthesis temperatures between 150-175 °C produced colors between cyan-yellow while temperatures of 225 °C and higher led to larger QDs. At 225 °C, longer hold times (3:00 min) led to larger QDs in comparison to shorter hold times (0:30 sec) at the same temperature. This shows that higher synthesis temperatures and longer hold times are two routes that can be taken to synthesize larger QDs. This can be further evidenced by recipe #5 which was done at 280 ° with 4:00 minutes of hold time which led to the largest QD diameters at all respective doping percentages. This may be

because of temperature on growth rate. As reaction temperature and growth rate are directly proportional, increasing hold time along with increasing growth rate will lead to larger QDs. For doping percentages of 0.05% and higher, PL quenching is consistent across all times and

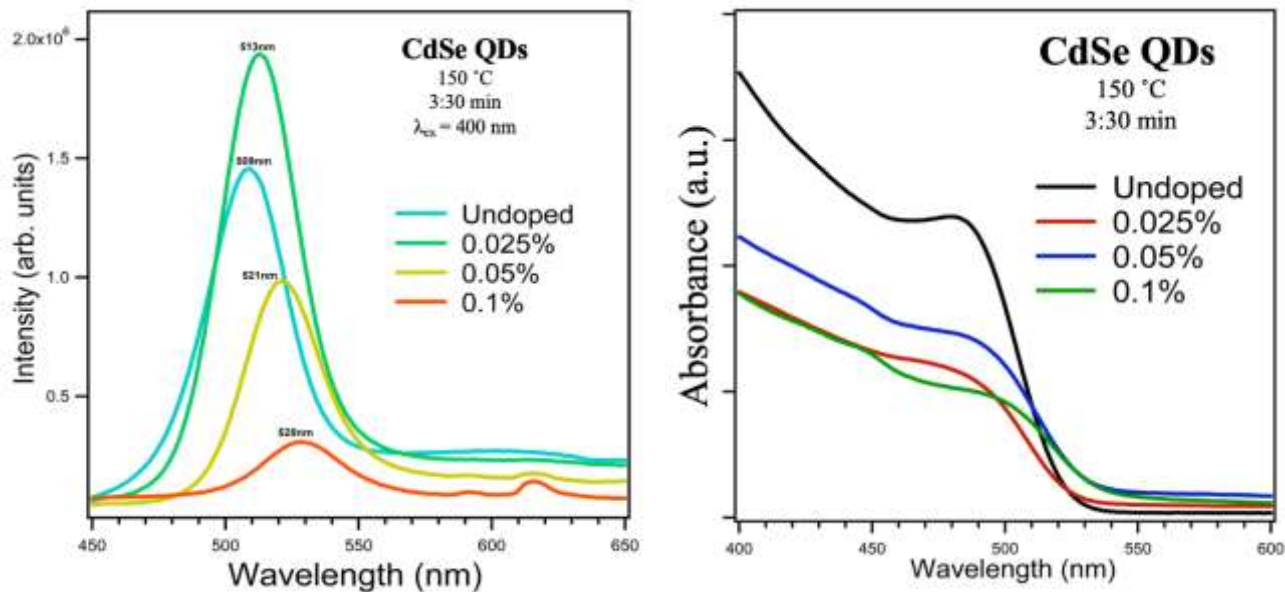


**Figure 3.** Photoluminescence (PL) data for CdSe QDs synthesized at 150 °C for 3:30 min, at all doping percentages (*left*). UV-VIS absorption data of the same quantum dots (*right*).

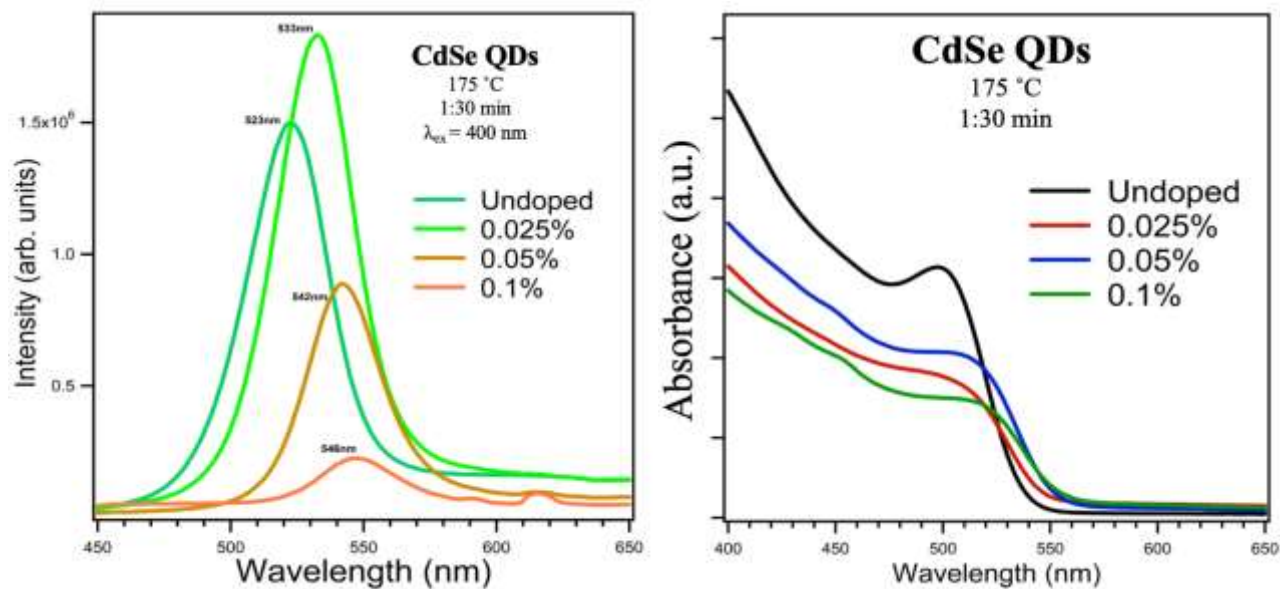


**Figure 4.** Photoluminescence (PL) data for CdSe QDs synthesized at 175 °C for 1:30 min, at all doping percentages (*left*). UV-VIS absorption data of the same quantum dots (*right*).

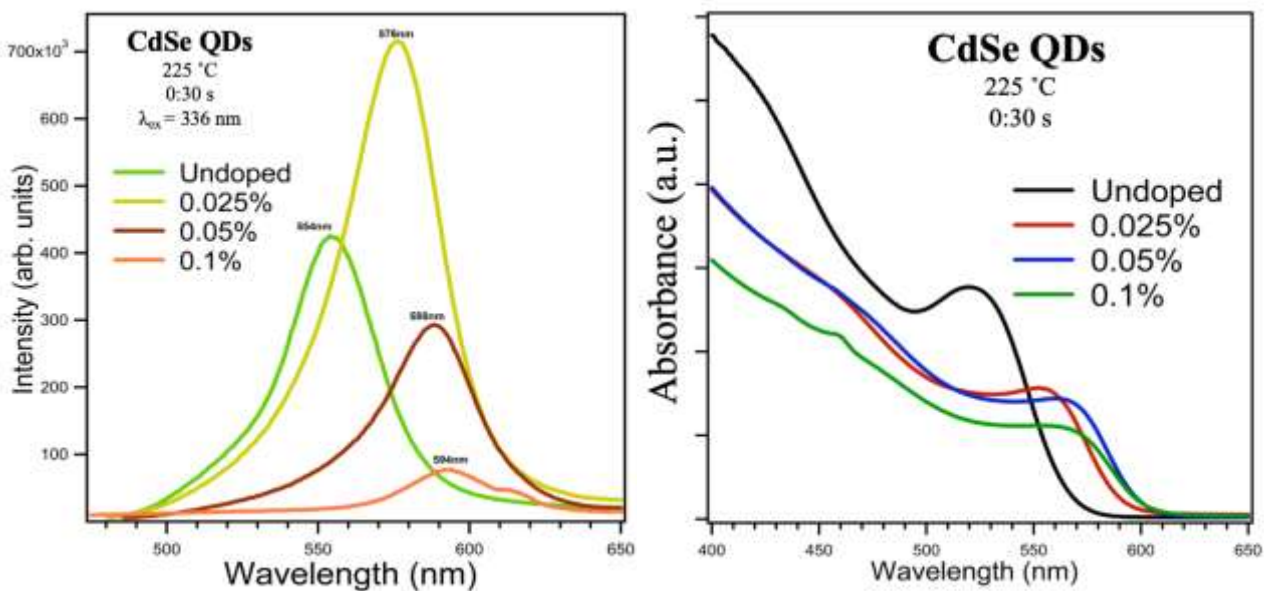


**Figure 5.** Photoluminescence (PL) data for CdSe QDs synthesized at 225 °C for 0:30 min, at all doping percentages (**left**). UV-VIS absorption data of the same quantum dots (**right**).

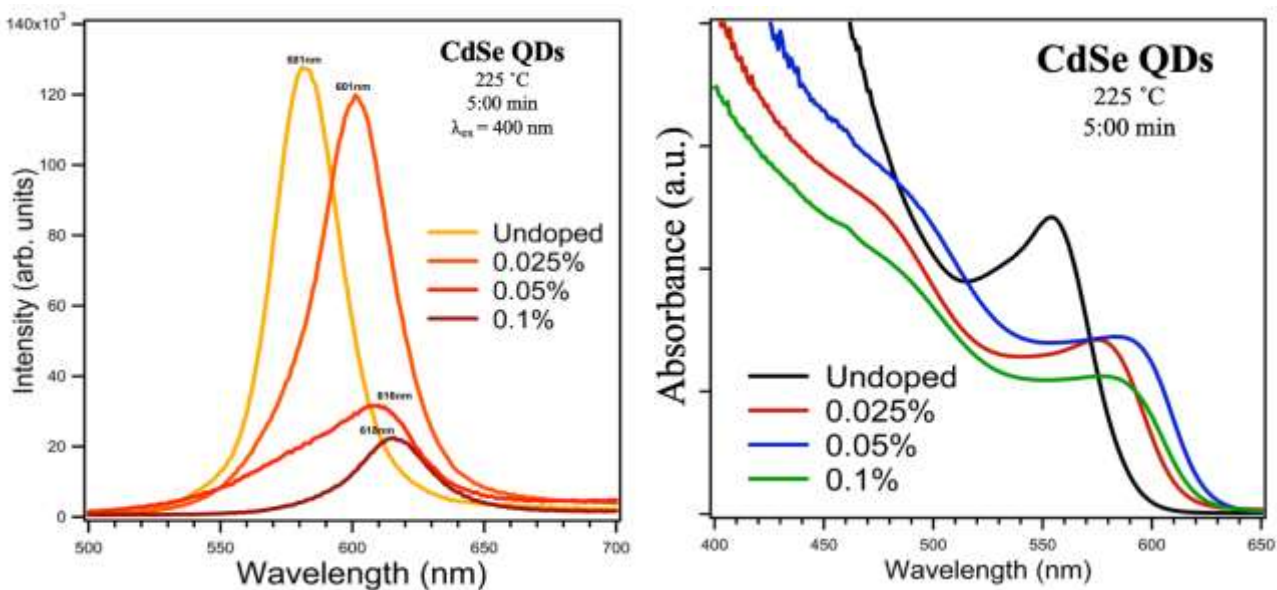


**Figure 6.** Photoluminescence (PL) data for CdSe QDs synthesized at 225 °C for 5:00 min, at all doping percentages (**left**). UV-VIS absorption data of the same quantum dots (**right**).

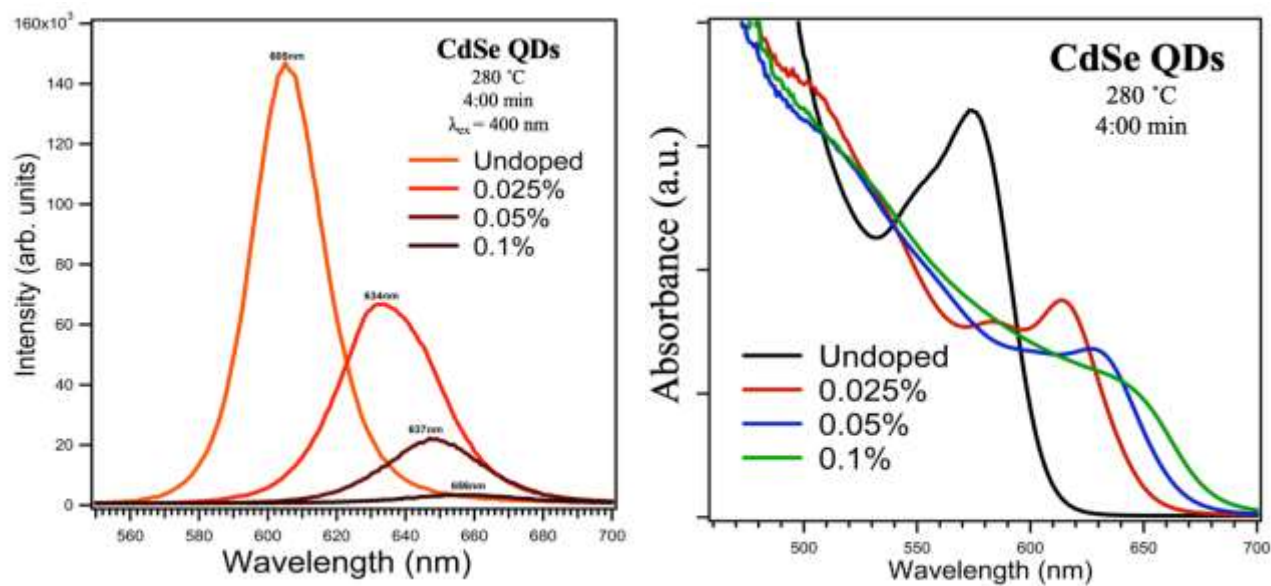


**Figure 7.** Photoluminescence (PL) data for CdSe QDs synthesized at 280 °C for 4:00 min, at all doping percentages (*left*). UV-VIS absorption data of the same quantum dots (*right*).

temperatures. This suggests that for those specific temperatures at 0.05% Eu<sup>3+</sup> doping and higher, surface attachment doping may be occurring as indicated by the formation of peaks from pure europium (III) acetate hydrate, while structural incorporation may be present for all other doped sample sets. When viewing the UV/Vis data, broadening of the absorption peak across all data sets as doping increases indicates that Eu<sup>3+</sup> ions are being structurally incorporated within the QD lattice.

### 3.3 Incorporation and Effects of Eu<sup>3+</sup> on Optoelectronic Properties

As mentioned earlier, the emission peaks observed at 579, 592, and 616 nm are the result of Eu<sup>3+</sup> doping. Literature reports each peak corresponds to separate transitions in Eu<sup>3+</sup> as visualized in Figure 8 [34]. Figure 8 displays the energy transfer process between CdSe and Eu<sup>3+</sup> that leads to Eu<sup>3+</sup> emission peaks observed in PL data [34-35]. The 579 nm emission peak

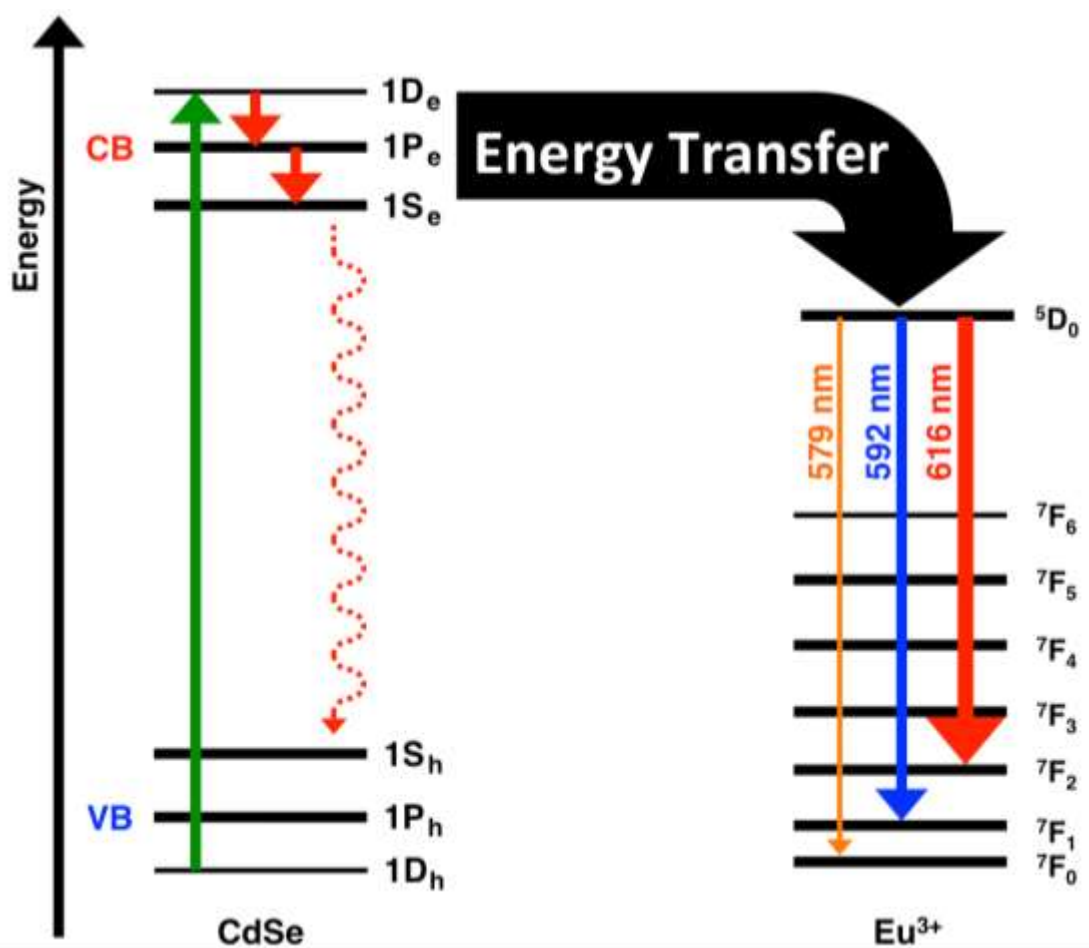


**Figure 8.** Energy transfer process between host CdSe and Eu<sup>3+</sup> dopant.

corresponds to the  ${}^5D_0 \rightarrow {}^7F_0$  transition while the 592 nm emission peak corresponds to the  ${}^5D_0 \rightarrow {}^7F_1$  transition, and the 616 nm peak that was consistent in all doped data sets is reported as the main Eu<sup>3+</sup> emission peak, which corresponds to the very strong  ${}^5D_0 \rightarrow {}^7F_2$  transition [36-38]. To further confirm the Eu<sup>3+</sup> peaks observed in the PL data, PL of pure europium (III) acetate hydrate dissolved in oleic acid and water were collected and is presented in Figure S4.1. Three Eu<sup>3+</sup> ion transition peaks are all present in both water and oleic acid. Furthermore, these peaks are present PL spectra of QDs, and the peak intensity is concentration dependent. The PL spectra not only show that QDs maintain the CdSe QDs intrinsic properties, but also exhibit the characteristic luminescence of Eu<sup>3+</sup> ions. Figure S4.2 presents normalized PL spectra to enhance the visibility of the Eu<sup>3+</sup> peaks when doped into QDs.

Lastly, the bandgap estimation method implord previously in previous studies was used for  $\text{Eu}^{3+}:\text{CdSe}$  QDs [24]. HOMO-LUMO calculation plots for each concentration of  $\text{Eu}^{3+}:\text{CdSe}$  are shown in Figures 9 along with bandgap values presented in Figure S5. Calculated QD diameters are fitted with standard deviation to display the discrepancy between the theoretically calculated

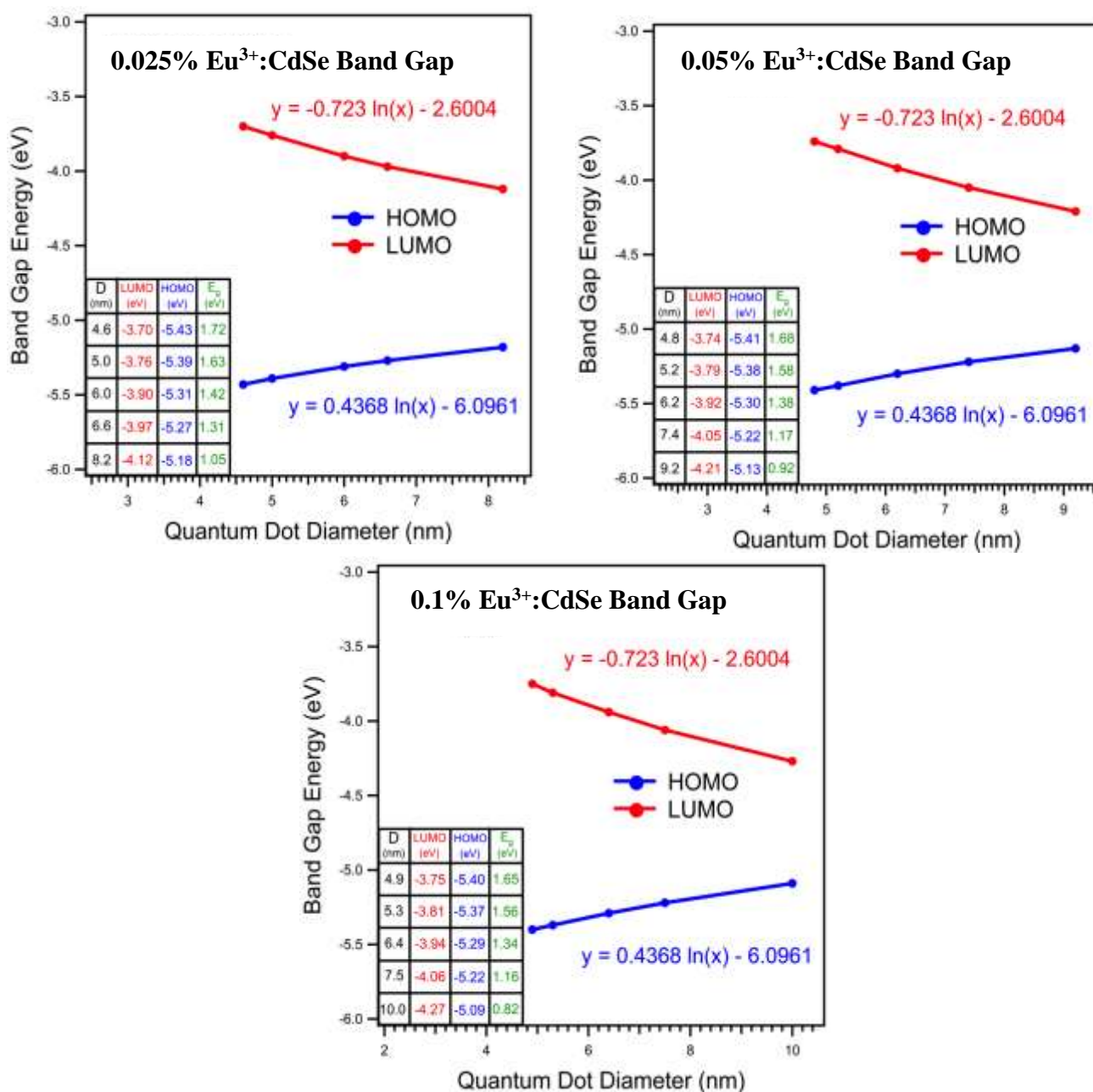


**Figure 9.** HOMO-LUMO level calculations for 0.025%  $\text{Eu}^{3+}:\text{CdSe}$  (left) and Band gap vs. QD diameter with standard deviation for 0.025%  $\text{Eu}^{3+}:\text{CdSe}$  (right).



diameter and experimental data. Plots show a wide deviation for larger quantum dots synthesized at higher temperatures and longer synthesis times. For each system, time and temperature variance do show to influence size and bandgap. A dopant material with an ionic radius similar to that of the host QD (among other factors) may undergo a structural incorporation mechanism [15]. When dopants are structurally incorporated into the lattice of a QD, PL quenching occurs as doping concentration increases and will be observed in PL spectra due to interstitial ion substitution [8-10,16-17]. As doping concentration and ion substitution increases towards the dopant maximum for this mechanism, the dopant begins to dominate and leads to this quenching of the quantum dot emission peak [18]. Exciton absorbance peaks may red or blue shift due to band gap shrinking or widening respectively, However, the most telling effect on UV-VIS data for structural incorporation is broadening and smearing of absorption peaks [8,19]. Figure 10 presents a schematic of the physical difference between structural incorporation and the surface attachment mechanism. These changes in absorbance peak shape due to ion doping can be a result of changes to the electronic band structure of the host QD material, such as narrowing of band edges which can cause QDs to change from direct to indirect band gap materials [20-21]. Emission within the quantum dot (as electrons relax back to the conduction band) provides energy to the dopants on

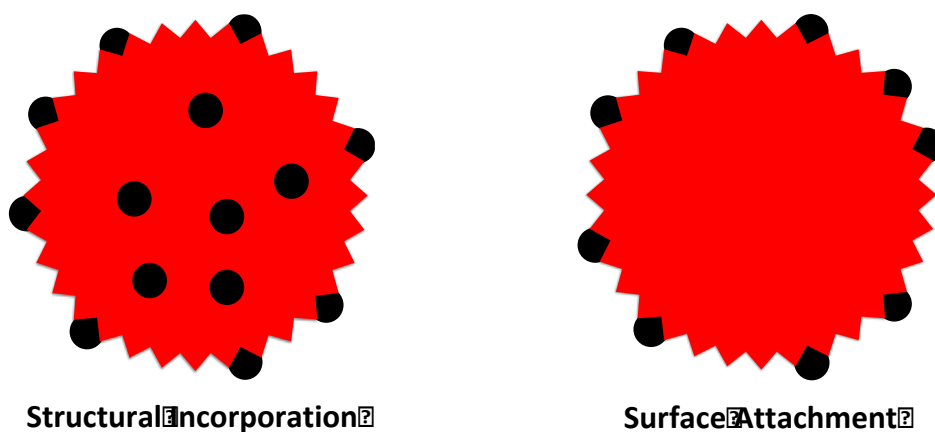


*Figure 10. Structural incorporation vs. surface attachment in quantum dot doping.*

the surface due to an energy transfer from the “donor” quantum dot to the “acceptor” dopant ion [24]. This causes fluorescence of the dopant ions on the surface, also known as photosensitized emission [25].

#### **4. CONCLUSION**

In conclusion,  $\text{Eu}^{3+}$  doped CdSe QDs were successfully synthesized using a simple, environmentally friendly, and single-step one-pot microwave synthesis method. Along with rapid synthesis, their optical properties were tuned by varying microwave irradiation temperatures, hold times, and dopant concentration.  $\text{Eu}^{3+}$  doped CdSe quantum dots had diameters ranging from 4.6 to 10.0 nm, with corresponding emission peaks from both the CdSe quantum dot and the  $\text{Eu}^{3+}$  ion suggesting that size can be tuned by doping at higher percentages and synthesis temperatures. The size of  $\text{Eu}^{3+}$  doped CdSe QDs at specific doping concentrations can also be tuned by varying hold time and temperature. UV-Vis absorption shows that Eu is incorporated into the lattice and affects the material's bandgap. We found that the introduction of dopant Eu in the CdSe QDs widens the optical absorption window compared to that of the un-doped QDs and this could be beneficial in applications such as QD solar cells. Considering the strong PL intensities and reproducibility of the CdSe-based QDs, they have potential use in doping other rare-earth ions. Rapid microwave synthesis is an economical, quick, and safe alternative to the “hot-injection” method with high throughput allowing QDs to be synthesized on a need-by-need basis. Implementation in optoelectronic devices such as solar cells and light-emitting diodes will be conducted in future studies.

#### **5. DATA AVAILABILITY**

The UV/Visible spectroscopy and photoluminescence data used to support the findings of this study are included within the article and in the supporting information.

## 6. CONFLICTS OF INTEREST

The authors declare no competing financial interest.

## 7. ACKNOWLEDGEMENTS

This work is supported by the National Science Foundation CREST grant numbers HRD-1036494, CREST-CREAM #HRD-1547771, and #HRD-1827214. Sandia National Laboratories is a multimission laboratory managed and operated by National Technology & Engineering Solutions of Sandia, LLC, a wholly-owned subsidiary of Honeywell International Inc., for the U.S. Department of Energy's National Nuclear Security Administration under contract DE-NA0003525. This paper describes objective technical results and analysis. Any subjective views or opinions that might be expressed in the paper do not necessarily represent the views of the U.S. Department of Energy or the United States Government.

## 8. REFERENCES

1. Glotzer, S. C. "Shape Matters." *Nature*, vol. 481, Jan. 2012
2. Hayden, D. R. "Biobased Nanoparticles for Broadband UV Protection with Photostabilized UV Filters." *American Chemical Society*, vol. 8, no. 48, Nov. 2016
3. Sousa Filho, P. "From Lighting to Photoprotection: Fundamentals and Applications of Rare Earth Materials." *Journal of the Brazilian Chemical Society*, vol. 26, no. 12, 2015
4. Linares-Avilés, Mariana. "Characterization of CBD-CdS Doped with Some Rare Earths III ( $\text{Eu}^{3+}$ ,  $\text{Ce}^{3+}$ ) as Function of Synthesis Time." *Materials Research*, vol. 21, no. 2, 2018
5. Ekamparam, S. "Effect of host-structure on the charge of europium ion." *Elsevier*, vol. 390, nos. 1-2, Mar. 2005
6. Li, W. "Color tunable organic light emitting diodes using Eu complex doping." *Elsevier*, vol. 51, Jan. 2007
7. Horoz, S. "Controlled synthesis of  $\text{Eu}^{2+}$  and  $\text{Eu}^{3+}$  doped ZnS quantum dots and their photovoltaic and magnetic properties." *AIP Advances*, vol. 6, Apr. 2016
8. Stavrinadis, A. "Aliovalent Doping in Colloidal Quantum Dots and Its Manifestation on Their Optical Properties: Surface Attachment versus Structural Incorporation." *Chemistry of Materials*, vol. 28, 2016
9. Papagiorgis, P. "The Influence of Doping on the Optoelectronic Properties of PbS Colloidal Quantum Dot Solids." *Scientific Reports*, vol. 6, Jan. 2016

10. Sugimoto, H. "Charge-Transfer-Induced Photoluminescence Enhancement in Colloidal Silicon Quantum Dots." *The Journal of Physical Chemistry C*, vol. 121, May 2017
11. Stavrinadis, A. "Strategies for the Controlled Electronic Doping of Colloidal Quantum Dot Solids." *ChemPhysChem*, vol. 17, 2016
12. Erwin, S. "Doping semiconductor nanocrystals." *Nature*, vol. 436, July 2005
13. Buonsanti, R. "Chemistry of Doped Colloidal Nanocrystals." *Chemistry of Materials*, vol. 25, no. 8, Mar. 2013
14. Bryan, J. "The Influence of Dopants on the Nucleation of Semiconductor Nanocrystals from Homogeneous Solution." *Journal of Nanoscience and Nanotechnology*, vol. 5, no. 9, Oct. 2005
15. Oreszczuk, K. "Origin of luminescence quenching in structures containing CdSe/ZnSe quantum dots with a few Mn<sup>2+</sup> ions." *Physical Review B*, vol. 96, Nov. 2017
16. Lommens, P. "Dopant Incorporation in Colloidal Quantum Dots: A Case Study on Co<sup>2+</sup> Doped ZnO." *Chemical Materials*, vol. 19, no. 23, Oct. 2007
17. Ain, N. "Tuning the Emission Energy of Chemically Doped Graphene Quantum Dots." *Nanomaterials*, vol. 6, no. 198, Oct. 2016
18. Hamizi, N. "Tunable optical properties of Mn-doped CdSe quantum dots synthesized via inverse micelle technique." *Optical Materials Express*, vol. 6, no. 9, Sept. 2016
19. Yang, W. "Adjusting the band structure and defects of ZnO quantum dots via tin doping†." *Royal Society of Chemistry*, vol. 7, 2017
20. Tavasoli, E. "Surface Doping Quantum Dots with Chemically Active Native Ligands: Controlling Valence without Ligand Exchange." *Chemistry of Materials*, vol. 24, no. 21, Oct. 2012
21. Yu, Y. "Enhanced emissions of Eu<sup>3+</sup> by energy transfer from ZnO quantum dots embedded in SiO<sub>2</sub> glass." *Nanotechnology*, vol. 19, no. 5, Jan. 2008
22. Ye, Y. "Charge-Transfer Dynamics Promoted by Hole Trap States in CdSe Quantum Dots–Ni<sup>2+</sup> Photocatalytic System." *Journal of Physical Chemistry C*, vol. 121, no. 32, July 2017
23. Chou, K. "Förster Resonance Energy Transfer between Quantum Dot Donors and Quantum Dot Acceptors." *Sensors*, vol. 15, no. 6, June 2015
24. Thomas, D.; Lee, H. O.; Santiago, K. C.; Pelzer, M.; Kuti, A.; Jenrette, E.; Bahoura, M. Rapid Microwave Synthesis of Tunable Cadmium Selenide (CdSe) Quantum Dots for Optoelectronic Applications. *J. Nanomater.* **2020**, 2020, 5056875.
25. Kwizera, P. "Synthesis and Characterization of CdSe Quantum Dots by UV-Vis Spectroscopy." *Macro to Nano Spectroscopy*, InTech, 2012
26. Uozumi, T. "Excited states of an electron-hole pair in spherical quantum dots and their optical properties." *American Physical Society*, Apr. 2002
27. Landes, C. "On the Nanoparticle to Molecular Size Transition: Fluorescence Quenching Studies." *Journal of Physical Chemistry B*, vol. 105, no. 43, Oct. 2001
28. Brus, L (1986). "Electronic Wave Functions in Semiconductor Clusters: Experiment and Theory". *The Journal of Physical Chemistry*. **90** (12): 2555–2560. doi:10.1021/j100403a003
29. Ekimov, A. I.; Hache, F.; Schanneklein, M. C.; Ricard, D.; Flytzanis, C.; Kudryavtsev, I. A.; Yazeva, T. V.; Rodina, A. V.; Efros, A. L. Absorption and Intensity-Dependent Photoluminescence Measurements on CdSe Quantum Dots. Assignment of the 1st Electronic-Transitions. *J. Opt. Soc. Am. B* 1993, 10, 100–107
30. Mao, H. "Photoluminescence investigation of CdSe quantum dots and the surface state effect." *Elsevier*, vol. 27, nos. 1-2, Mar. 2005

31. Kwizera, P. "Synthesis and Characterization of CdSe Quantum Dots by UV-Vis Spectroscopy." *Macro to Nano Spectroscopy*, InTech, 2012
32. Kippeny, T. "Semiconductor Nanocrystals: A Powerful Visual Aid for Introducing the Particle in a Box." *Journal of Chemical Education*, vol. 79, no. 9, Sept. 2002
33. Binnemans, K. "Interpretation of europium(III) spectra." *Elsevier*, vol. 295, no. 1, July 2015.
34. Xiao, X. "Cell assay using a two-photon-excited europium chelate." *Biomedical Optics Express*, vol. 2, no. 8, Aug. 2011
35. Reyes, R. "Growth and Characterization of OLED's with Europium Complex as Emission Layer." *Brazilian Journal of Physics*, vol. 32, no. 2B, June 2002.
36. Carreira, L. "Europium (III) ion probe spectrofluorometric determination of diclofenac sodium." *Elsevier*, vol. 13, no. 11, Oct. 1995.
37. He, Q. "Luminescent Europium Chelates Synthesis and Fluorescence Properties." *Sensors and Materials*, vol. 19, no. 2, Mar. 2007.
38. He, G. " Multi-photon excitation properties of CdSe quantum dots solutions and optical limiting behavior in infrared range." *Optics Express*, vol. 15, no. 20, Sep. 2007